PCCP

1,2,3-Benzodithiazolyl radicals formed by thermolysis and photolysis of 1,3,2,4-benzodithiadiazines

Ivan V. Vlasyuk,†[ab] Victor A. Bagryansky,*[ab] Nina P. Gritsan,[ab] Yuri N. Molin,[ab] Alexander Yu. Makarov,[c] Yuri V. Gatilov,[c] Vladimir V. Shcherbukhin[d] and Andrey V. Zibarev*[c]

[a] *Institute of Chemical Kinetics and Combustion, Siberian Branch of Russian Academy of Sciences, 630090 Novosibirsk, Russia. E-mail: vbag@ns.kinetics.nsc.ru*
[b] *Novosibirsk State University, 630090 Novosibirsk, Russia*
[c] *Institute of Organic Chemistry, Siberian Branch of Russian Academy of Sciences, 630090 Novosibirsk, Russia. E-mail: zibarev@nioch.nsc.ru*
[d] *Institute of Organic Chemistry, Russian Academy of Sciences, 117913 Moscow, Russia*

Received 17th October 2000, Accepted 30th November 2000
First published as an Advance Article on the web 9th January 2001

Mild thermolysis (at 110–150 °C) of 1,3,2,4-benzodithiadiazine **1** and its carbocyclic substituted derivatives **2**–**15** in hydrocarbon solvents quantitatively yields stable 1,2,3-benzodithiazolyl π-radicals **1**$^\bullet$–**15**$^\bullet$. Kinetics of this reaction can be described as a first-order process. Arrhenius parameters of the effective rate constant are $E_a = 80 \pm 8$ kJ mol^{-1}, $k_0 = 10^{6.4 \pm 1.1}$ s^{-1} for **1** in squalane. Room-temperature photolysis of **1** in hydrocarbon solvents also affords radical **1**$^\bullet$ in nearly quantitative yield. Quantum yield of photolysis is wavelength dependent and is equal to 0.08 ± 0.01 at 313 nm in benzene. Experimental hyperfine coupling (hfc) constants in the ESR spectra of **1**$^\bullet$–**15**$^\bullet$ agree fairly well with those calculated at the B3LYP/CC-pVDZ level of theory. Spin density distribution in **1**$^\bullet$–**15**$^\bullet$ is in striking contrast to that of isomeric 1,3,2-benzodithiazolyls but resembles the distribution in correspondingly substituted benzyl radicals. ESR linewidths of radicals **1**$^\bullet$-**15**$^\bullet$ display some features likely related to spin-rotational relaxation.

Introduction

The design and synthesis of organic molecules with high-spin ground states (molecular magnets)[1,2] is of obvious fundamental significance. A rational approach to designing high-spin molecules consists of conceptually dividing the molecule into two components: a spin-containing (SC) fragment which provides the unpaired electron, and a ferromagnetic coupling (FC) unit which connects radical centers ferromagnetically.[3]

Among the potential building blocks, the heterocyclic sulfur–nitrogen π-radicals (SCs) attached in various ways to aromatic rings (FCs), for example **A**–**C** (Scheme 1), belong to the most promising ones.[4,5] For instance, a system with the **A** derivative (Ar = 4-CNC$_6$F$_4$) displays spontaneous magnetization at 36 K[6] (*cf.* the other known molecular ferromagnets 2). The source of unpaired electrons in all these radicals is a two-atom three-π-electron fragment (SN)$^\bullet$,[3] *i.e.* the same moiety that the well-known molecular metal and low-temperature superconductor poly(sulfur nitride) (SN)$_x$[7] is composed of.

At the same time, while 4-Ar-1,2,3,5-dithiadiazolyls **A**, 1,3,2-benzodithiazolyls **B**, and the corresponding multiradicals have been isolated and extensively studied in both liquid and solid phases,[4] 1,2,3-benzodithiazolyls **C**, isomers of **B**, have only been briefly investigated in solution.[4,8] The reason for this is that the traditional approach to **C** radicals mainly based on the reduction of the Herz salts (1,2,3-arenodithiazolium chlorides[9]),[8,10] and the thermolysis and photolysis of rare sulfur–nitrogen compounds [3*H*-1,2,3-benzodithiazol-2-oxide, (PhNH)$_2$S, PhN(SR)$_2$ where *R* = piperid-1-yl, *etc.*][8,11,12] affords target radicals in low yields[8–12] along with numerous by-products.

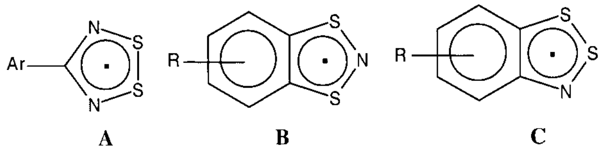

A **B** **C**

Scheme 1

We found that mild (~110–150 °C) thermolysis and photolysis of the newly synthesised 1,3,2,4-benzodithiadiazines (Scheme 2)[13–16] in dilute hydrocarbon solutions resulted in nearly quantitative yields of **C** radicals (for preliminary work, see ref. 17). The present paper describes in detail the preparation and ESR characterisation of a large number of novel 1,2,3-benzodithiazolyls **C** based on this new approach. The data obtained could be useful for designing synthetic pathways to 1,2,3-benzodithiazolyl-based multiradicals with potentially ferromagnetic properties.

Experimental

The 1,3,2,4-benzodithiadiazines **1**–**15** were synthesised and purified as reported previously.[13–16] Thermolysis or photolysis of their 10^{-3} M solutions in absolute hydrocarbon solvents [2,6,10,15,19,25-hexamethyltetracosane (squalane), nonane,

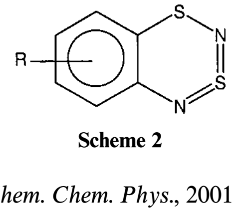

Scheme 2

---

† Present address: Department of Chemistry and Biochemistry, New Mexico State University, Las Cruces, NM, USA.

DOI: 10.1039/b008408p

hexane, cyclohexane, benzene, and *trans*-decalin] was performed in an ESR Teflon valve-equipped quartz tube outgassed by three freeze–pump–thaw cycles.

The thermolysis was carried out with a glycerol thermostat in a temperature range of 110–150 °C, with a temperature accuracy of ±0.5 °C. In a typical experiment, a solution of the radical precursor was gradually heated to 150 °C. After keeping for 1 h at this temperature, the sample was cooled to 20 °C, and the ESR spectrum was measured. In squalane, detectable amounts of radicals appeared at 110 °C, whereas in cyclohexane they appeared even at 90 °C.

The photolysis was performed using the selected lines of a Hg lamp (DRSh-500) equipped with a water filter. To isolate individual lines (313, 365, 436 nm), combinations of glass filters were employed. The UV/VIS spectra were collected on a Specord M40 instrument. The quantum yields of the photolysis were determined using 2-dimethylamino-3-chloro-1,4-naphthoquinone as the standard with a quantum yield of isomerization of 0.1 in benzene.[18]

The ESR spectra were recorded on a Bruker EMX spectrometer (MW power 0.64 mW, modulation frequency 100 kHz, modulation amplitude 0.01 mT). The spectra integration and simulation were performed with the WIN-EPR, Simfonia, WinSim and NIEHS PEST software programs. The *g*-factors of radicals were measured using a DPPH standard.

The conversion of precursors into radicals was determined by a $CuCl_2 \cdot 2H_2O$ standard with an accuracy of ±15%.

The B3LYP/6-31G* and B3LYP/CC-pVDZ calculations were carried out by means of the GAUSSIAN 94 program.[19] The electronic absorption spectra were calculated using the time-dependent density functional theory at the TD-B3LYP/6-31+G* level with the Gaussian 98 suite of programs.[20]

1,3,2-Benzodithiazolyl **16**˙ (Scheme 1: **B**, R = H), an isomer of **1**˙, was prepared by reduction of 1,3,2-benzodithiazolium chloride[21] with Ph_3Sb. The ESR spectrum corresponded to the published spectrum[21] with a slightly better resolution.

Results and discussion

The heteroatom reactivity of the newly synthesized 1,3,2,4-benzodithiadiazines (which exhibit some formal features of antiaromaticity, for details see ref. 13–16 and references cited therein) is poorly known. Nevertheless, it seems to be high and varied.[13–16,22] It is believed that many new reactions will be observed, and many new structural types will be found among the reaction products of 1,3,2,4-benzodithiadiazines. Reasonably, the first step in studying the chemistry of these compounds is the investigation of their thermal stability and the identification of decomposition products.

Although photochemical methods are used for synthetic purposes rather rarely, they provide wide opportunities for studying the mechanisms of the processes. The methods of laser flash and low-temperature photolysis in combination with those of matrix isolation very frequently give direct information about reaction intermediates, their properties and reactivity. In the case where both thermolysis and photolysis result in identical products, it is assumed that the reaction intermediates in these processes will be the same. This can contribute much to the understanding of the mechanism of thermal transformations. Therefore, along with the thermolysis of 1,3,2,4-benzodithiadiazines **1**–**15**, the photolysis of the parent compound **1** in a series of hydrocarbon solvents (squalane, hexane, benzene) was also performed at room temperature in order to elucidate the nature of photolysis products and determine photo-transformation efficiency.

Thermolysis of 1,3,2,4-benzodithiadiazines

We found that mild (~110–150 °C) thermolysis of 1,3,2,4-benzodithiadiazines **1**–**15** in hydrocarbon solvents (squalane, nonane, hexane, cyclohexane, benzene, or *trans*-decalin) resulted in stable radicals **1**˙–**15**˙ (Scheme 3; Table 1). Fig. 1 presents the ESR spectrum of **1**˙ prepared by 1-h thermolysis of **1** at 150 °C in squalane and hexane. Fig. 2 depicts spectra of **4**˙–**7**˙, **9**˙, **13**˙–**15**˙ generated from the corresponding precursors

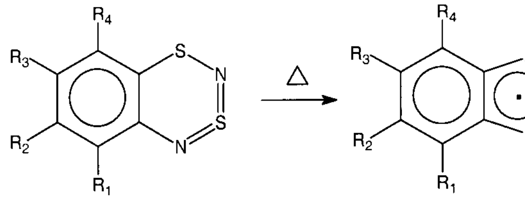

1 – 15 **1**˙**- 15**˙

for $R_1 - R_4$ see Table 1

Scheme 3

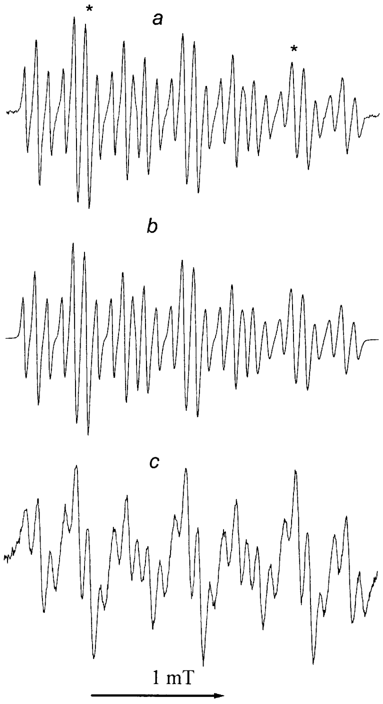

Fig. 1 ESR spectrum of radical **1**˙: *a*, experimental in squalane; *b*, simulated with hfc constants (Table 2) and linewidths best fitting curve *a*; *c*, experimental in hexane. Asterisks denote the lines for which Fig. 7 shows the dependence of width on solvent viscosity.

Table 1 Carbocyclic substituents in **1**˙–**15**˙[a]

Radical	R_1	R_2	R_3	R_4
1˙	H	H	H	H
2˙	H	H	OCH_3	H
3˙	H	H	CH_3	H
4˙	H	F	H	H
5˙	H	H	F	H
6˙	F	F	F	F
7˙	H	Br	H	Br
8˙	H	H	Br	H
9˙	CF_3	H	H	H
10˙	H	H	Cl	H
11˙	OCH_3	H	H	H
12˙	H	CH_3	H	H
13˙	Br	H	H	H
14˙	H	Br	H	H
15˙	H	H	H	Br

[a] For the precursors **1**–**15**, R_1–R_4 are the same (see Scheme 3).

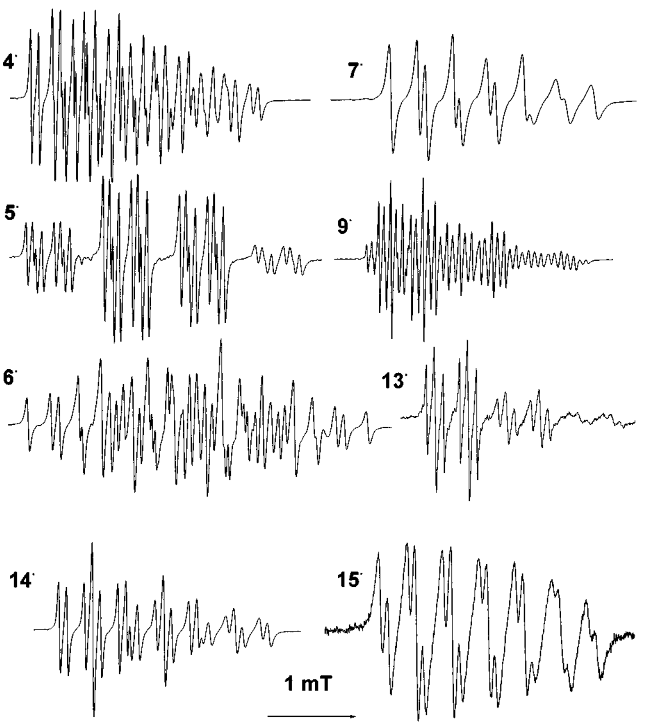

Fig. 2 ESR spectra of radicals **4**$^{\cdot}$–**7**$^{\cdot}$, **9**$^{\cdot}$, **13**$^{\cdot}$–**15**$^{\cdot}$ in squalane.

under the same conditions. For **1**$^{\cdot}$, the identical spectrum was obtained by thermolysis in other solvents, as well as by reduction of 1,2,3-benzodithiazolium chloride[9,16] with Ph_3Sb in toluene at 20 °C.

The obtained ESR spectra of 1,2,3-benzodithiazolyl (**1**$^{\cdot}$) and some of its carbocyclic substituted derivatives **2**$^{\cdot}$, **3**$^{\cdot}$, **8**$^{\cdot}$, **10**$^{\cdot}$–**12**$^{\cdot}$ are identical with those,[8–12] prepared by other methods, mainly by reduction of the corresponding Herz salts by metal powders. One can conclude that the thermolysis of **1**–**15** solutions affords 1,2,3-benzodithiazolyl π-radicals. The radicals **4**$^{\cdot}$–**7**$^{\cdot}$, **9**$^{\cdot}$, **13**$^{\cdot}$–**15**$^{\cdot}$ are synthesised for the first time. Thus, this approach is superior to methods reported previously.[8–12] In particular, the Herz salts corresponding to **4**$^{\cdot}$–**7**$^{\cdot}$, **9**$^{\cdot}$, **13**$^{\cdot}$–**15**$^{\cdot}$ have not yet been described.[9]

All the ESR spectra obtained are well resolved. The width of individual lines lies in the range 0.03–0.05 mT depending on the solvent and position in the spectra. The hyperfine coupling (hfc) constants with all magnetic nuclei presented are reliably determined by fitting (for example, see Fig. 1, curve *b*), in which the hfc constants and linewidths are varied independently. Table 2 contains the experimental hfc constants for **1**$^{\cdot}$–**15**$^{\cdot}$ along with the theoretical values calculated at the B3LYP/CC-pVDZ level of theory. For novel radicals **4**$^{\cdot}$–**7**$^{\cdot}$, **9**$^{\cdot}$, **13**$^{\cdot}$–**15**$^{\cdot}$ the values of hfc constants with nitrogen and hydrogen nuclei are close to those of the known 1,2,3-benzodithiazolyls, verifying the assigned structure.

It should be noted that radical **1**$^{\cdot}$ and its derivatives were initially assigned to the 1,2-benzothiazetyl structure[11,23] [*i.e.* with the (SN)$^{\cdot}$, not the (SSN)$^{\cdot}$, fragment connected to the 1,2-positions of the aromatic ring]. The assignment was subsequently corrected to 1,2,3-benzodithiazolyl on the basis of ESR experiments with the ^{33}S-enriched species. These experiments indicated the presence of two non-equivalent sulfur atoms.[8] The 1,2,3-benzodithiazolyl structure is also consistent with the fact that the radicals can be oxidised to Herz salts by molecular chlorine.[12]

The assignment of hfc constants in **1**$^{\cdot}$–**15**$^{\cdot}$ (Table 2) is based on earlier data,[8,11,12,23] substitutional effects and the results of the B3LYP/CC-pVDZ calculations of spin density distribution. The molecular structure of the parent radical **1**$^{\cdot}$ optimised at the B3LYP/6-31G* level of theory is presented in Fig. 3. The calculated constants are consistent with the experimental data (Table 2). Of interest is the similarity of the relative values of the hfc constants of radicals **1**$^{\cdot}$–**3**$^{\cdot}$ and those of the correspondingly substituted benzyl radicals 4-RC_6H_4–$CH_2^{\cdot}$ (R = H, OCH_3, CH_3).[24] For instance, the character of hfc values distribution over the ring in the C_6H_5–$CH_2^{\cdot}$ radical is the same as that in **1**$^{\cdot}$. One can conclude then that the 1,2,3-benzodithiazolyls are the hetero-analogs of benzyl radicals in their spin density distribution.

On the other hand, the spin density distribution in **1**$^{\cdot}$ is in striking contrast to that of the isomeric 1,3,2-benzodithiazolyl **16**$^{\cdot}$ (for B3LYP/CC-pVDZ data, see Scheme 4). The ESR spectrum of **16**$^{\cdot}$ consists of a 1 : 1 : 1 triplet with almost no hyperfine splitting due to spin coupling with protons.[21] We measured (calculated) the following values: $a^N = 1.14$ (1.05),

Table 2 Hfc constants (in parentheses, theoretical values) and *g*-factors of radicals **1**$^{\cdot}$–**15**$^{\cdot}$

Radical	Hfc constants/mT					*g*-fact
1$^{\cdot}$	N: 0.82 (0.80)	H(1): 0.29 (−0.26)	H(2): 0.08 (0.11)	H(3): 0.37 (−0.30)	H(4): 0.10 (0.12)	2.0080
2$^{\cdot}$	N: 0.86 (0.83)	H(1): 0.29 (−0.23)	H(2): 0.04 (0.08)	3H(OCH_3): 0.05 (0.06)	H(4): 0.11 (0.12)	2.0076
3$^{\cdot}$	N: 0.84 (0.81)	H(1): 0.30 (−0.25)	H(2): 0.08 (0.11)	3H(CH_3): 0.39 (0.32)	H(4): 0.10 (0.12)	2.0076
4$^{\cdot}$	N: 0.79 (0.77)	H(1): 0.24[a] (−0.23)	F(2): 0.27[a] (−0.33)	H(3): 0.39 (−0.31)	H(4): 0.090 (0.11)	2.0081
5$^{\cdot}$	N: 0.86 (0.82)	H(1): 0.32 (−0.27)	H(2): 0.07 (0.10)	F(3): 0.85 (0.95)	H(4): 0.11 (0.12)	2.0079
6$^{\cdot}$	N: 0.82 (0.80)	F(1): 0.57 (0.72)	F(2): 0.26 (−0.36)	F(3): 1.00 (1.00)	F(4): 0.35 (−0.41)	2.0078
7$^{\cdot}$	N: 0.78	H(1): 0.31	Br: < 0.01	H(3): 0.40	Br: < 0.01	—
8$^{\cdot}$	N: 0.80	H(1): 0.30	H(2): 0.10	Br: < 0.01	H(4): 0.08	—
9$^{\cdot}$	N: 0.77 (0.75)	3F(CF_3): 0.14 (0.15)	H(2): 0.08 (0.09)	H(3): 0.36 (−0.29)	H(4): 0.06 (0.10)	—
10$^{\cdot}$	N: 0.80 (0.79)	H(1): 0.30 (−0.26)	H(2): 0.09 (0.11)	Cl: < 0.01	H(4): 0.10 (0.12)	—
11$^{\cdot}$	N: 0.82 (0.80)	3H(OCH_3): 0.03 (0.05)	H(2): 0.11 (0.12)	H(3): 0.38 (−0.30)	H(4): 0.10 (0.11)	—
12$^{\cdot}$	N: 0.81	H(1): 0.28	3H(CH_3): 0.08	H(3): 0.38	H(4): 0.10	—
13$^{\cdot}$	N: 0.80	Br: < 0.01	H(2): 0.10	H(3): 0.37	H(4): 0.09	—
14$^{\cdot}$	N: 0.80	H(1): 0.29	Br: < 0.01	H(3): 0.38	H(4): 0.09	—
15$^{\cdot}$	N: 0.80	H(1): 0.32	H(2): 0.10	H(3): 0.39	Br: < 0.01	—

[a] Interchangeable values.

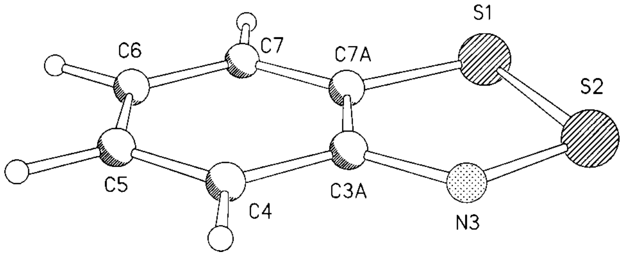

Fig. 3 B3LYP/6-31G* geometry of radical **1**$^{\bullet}$. Selected bond lengths (Å) and bond angles (°): C7aS1 1.765, S1S2 2.149, S2N3 1.647, N3C3a 1.355, C3aC7a 1.434, C3aC4 1.418, C4C5 1.384, C5C6 1.406, C6C7 1.394, C7C7a 1.396; C7aS1S2 90.3, S1S2N3 99.0, S2N3C3a 115.1, N3C3aC7a 120.3, S1C7aC3a 115.4. The radical is perfectly planar.

$a^{H4(H7)} = 0.05\ (-0.04)$, $a^{H5(H6)} = 0.05\ (-0.02)$, mT. Thus, most of the spin density of **16**$^{\bullet}$ is localized on the heterocyclic five-membered ring.

The radicals studied display the absence of hfc with Cl (**10**$^{\bullet}$) and Br (**7**$^{\bullet}$, **8**$^{\bullet}$, **13**$^{\bullet}$–**15**$^{\bullet}$) nuclei. A similar feature of Cl and Br substituents was observed in substituted benzyl radicals.[25] Practically, this property can be used to switch-off the proton's hfc in known positions (in particular, the structure of the precursors **8**, **13**–**15** of the radicals **8**$^{\bullet}$, **13**$^{\bullet}$–**15**$^{\bullet}$ was unambiguously determined by X-ray crystallography[16]). Usually, the more laborious method of isotopic labelling, for example with deuterium, is used for these purposes.

The kinetics of radical accumulation upon thermolysis of **1** in squalane (Fig. 4) can be approximated by the first-order equation

$$A(t) = B(1 - e^{-kt}) \qquad (1)$$

where B is the concentration of radicals at $t = \infty$, and k is the effective rate constant. The rate constant k was measured in

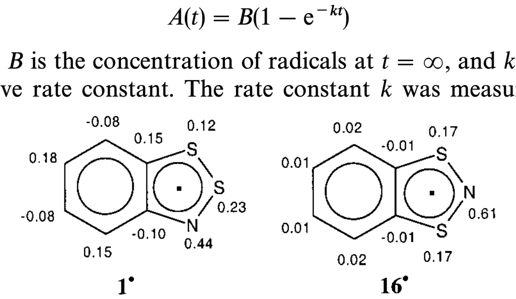

1$^{\bullet}$

16$^{\bullet}$

Scheme 4

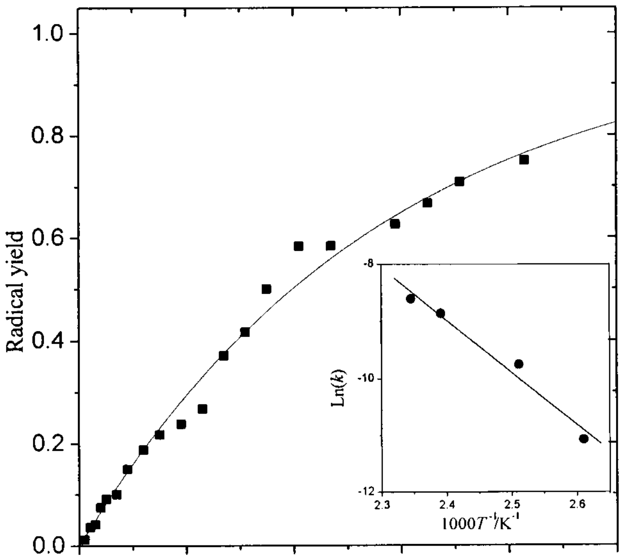

Fig. 4 Kinetics of radical **1**$^{\bullet}$ formation upon thermolysis of a solution of **1**$^{\bullet}$ in squalane at $T = 125\,°C$ (initial concentration of **1** was equal to 10^{-3} M). Inset: Arrhenius plot of the formation rate constant of **1**$^{\bullet}$ in squalane.

the temperature range 110–150 °C and was found to fit well with the Arrhenius law (Fig. 4, inset). The activation energy was found to be $E_a = 80 \pm 8$ kJ mol^{-1} and the pre-exponential factor $k_0 = 10^{6.4 \pm 1.1}$ s^{-1}.

Our measurements indicate the nearly quantitative conversion of **1**–**15** into **1**$^{\bullet}$—**15**$^{\bullet}$ For example, 1 h thermolysis of **1** at 145 °C affords **1**$^{\bullet}$ in 95% yield (in squalane). However, further heating leads to a slow decrease of radical concentration.

Radicals **1**$^{\bullet}$–**15**$^{\bullet}$ at ambient temperature in oxygen-free hydrocarbon solutions are very stable. After 3 weeks the concentrations of **1**$^{\bullet}$–**15**$^{\bullet}$ in air-protected squalane solutions decreased by only 30%. In the presence of oxygen, the radicals are less stable, especially under heating. Thus, in air-saturated squalane solutions at 150 °C, the ESR signal completely decays in 5 min.

The removal of the hexane solvent by low-temperature distillation in vacuum also leads to ESR signal disappearance. However, upon dissolving the residue, the ESR signal is regained which testifies to the formation of weakly bound diamagnetic dimers in the solid state, typical of many heterocyclic sulfur–nitrogen radicals including those of type **B**.[4,26]

Photolysis of 1,3,2,4-benzodithiadiazines

Fig. 5 shows the experimental electronic absorption spectrum of **1** characterized by a number of bands in the visible and UV regions, along with the theoretical spectrum calculated at the time dependent B3LYP/6-31+G* level. It is clear that the experimental spectrum is well reproduced by the time-dependent density functional theory.

The theoretical spectrum of **1** was calculated for the geometry optimized by the B3LYP/6-31G* method. According to the calculations, the heterocycle of **1** is bent along the S1–N4 line by about 15°. We have also calculated the spectrum for a planar geometry of the heterocycle. The calculated spectrum is close to that of Fig. 5 in the energy of transitions, but differs in their intensities. Therefore, although the geometry of the free molecule of **1** is non-planar, and the calculations involve the Kohn–Sham orbitals, we have characterized the absorption bands as ππ* and πσ*. The long-wavelength band at 616 nm and the two bands in the near-UV region are of the ππ* type. The transition at 314 nm can be assigned to the πσ* type.

Prolonged irradiation of **1** solution by visible light (>400 nm) does not cause any noticeable photo transformation. UV irradiation of the solution (365 or 313 nm) leads to a significant change in the electronic absorption spectrum. In this

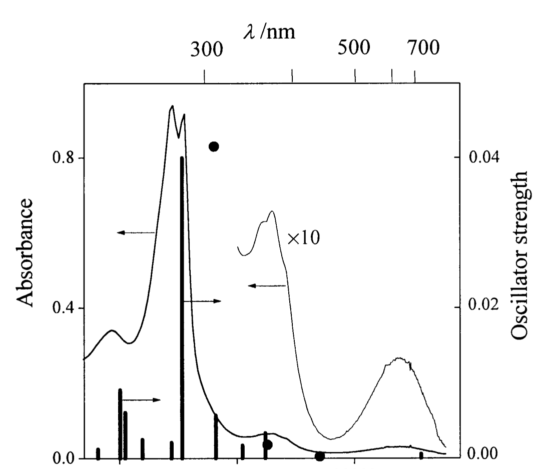

Fig. 5 Experimental and calculated (vertical lines, TD-B3LYP) electronic absorption spectrum of **1**. Points, quantum yields (φ) of **1** photo decomposition ($\varphi = 0.08$ at 313 nm in benzene) at different wavelengths.

case, the ESR spectrum of the sample accumulates a signal identical with that of radical **1**$^{\bullet}$ (Fig. 1). The UV/VIS spectrum of **1**$^{\bullet}$ measured in this work corresponds to the previously reported spectrum.[8]

Fig. 6 presents the kinetics of radical **1**$^{\bullet}$ accumulation under irradiation of a solution of **1**. It is seen that the yield of radicals amounts to 90%. Under further irradiation, the radicals vanish during the secondary photochemical reactions. In the absence of radical photo transformation, the yield is expected to be close to 100%. The quantum yield of photolysis of **1** at 313 nm is equal to 0.08 ± 0.01 in benzene and 0.15 ± 0.01 in hexane. When **1** is irradiated by the 365 nm light, the quantum yield decreases more than 20 times (Fig. 5). This dependence of quantum yield on the irradiation wavelength testifies to the fact that a highly excited electronic state of **1** (see Fig. 5) is responsible for its photo-transformation under discussion.

The transformation of **1**–**15** into **1**$^{\bullet}$–**15**$^{\bullet}$ is not trivial, requiring ring contraction with a loss of the N atom. The reaction probably proceeds through the singlet 1,2,3-benzodithiazol-2-ylnitrenes (Scheme 5), the isomers of **1**–**15**. The detailed data on stationary and laser flash photolysis, matrix isolation study and non-empirical quantum chemical calculations to support the proposed mechanism (Scheme 5) will be presented elsewhere[27] (for preliminary work, see ref. 17(*b*)). Here it is only necessary to note that the nitrene hypothesis is consistent with the heteroatom reactivity of **1**–**15** towards Ph_3P[22] and SCl_2[16] to give the products of the oxidative imination of phosphorus and sulfur, respectively (Scheme 6).

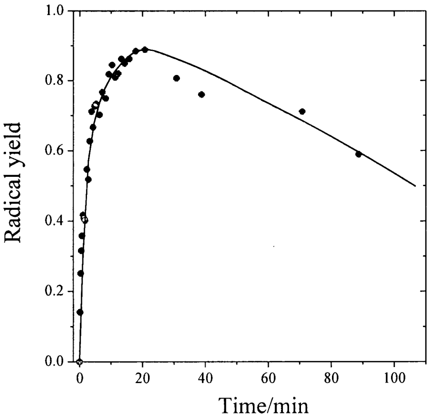

Fig. 6 Kinetics of radical **1**$^{\bullet}$ formation and decay under irradiation of **1** in squalane by 313 nm light.

Some features of spin relaxation of 1,2,3-benzodithiazolyls

The low ($<10^{-5}$ M) radical concentrations were used to eliminate the line broadening due to spin exchange and to increase the spectral resolution. Among the solvents used, the most resolved but slightly asymmetric ESR spectra of radicals **1**$^{\bullet}$–**15**$^{\bullet}$ were obtained in the most viscous, squalane ($\eta = 21$ cP). The asymmetry testifies to a noticeable contribution to the rate of paramagnetic relaxation from the modulation of hfc and *g*-tensor anisotropy by tumbling rotation. This contribution is proportional to solvent viscosity.[28] In the less viscous solvents, *e.g.* hexane ($\eta = 0.31$ cP), the spectral asymmetry vanishes but the spectral lines broaden (Fig. 1). The broadening indicates the prevailing contribution of spin-rotational relaxation, which gives the inversely proportional dependence of linewidth on viscosity.[29] Since an increase in linewidth with decreasing solvent viscosity is rather uncommon, it was studied additionally.

Fig. 7 shows the dependence of the widths of the two lines of the radical **1**$^{\bullet}$ spectrum, denoted in Fig. 1 by asterisks, on solvent viscosity. As the viscosity increases, the widths of both lines decrease. At high viscosity, the width of the high-field line slowly increases.

The smooth curves in Fig. 7 correspond to the optimum description of the dependence of the experimental linewidth ΔH_{pp} on viscosity η in terms of the equation

$$\Delta H_{pp} = a + b/\eta + c\eta \qquad (2)$$

with the additional condition that parameters *a* and *b* are the same for both lines. In eqn (2) parameter *a* characterizes the contribution of viscosity-independent relaxation mechanisms to the linewidth; parameter *b* characterizes the contribution of spin-rotational interaction; and parameter *c* characterizes the

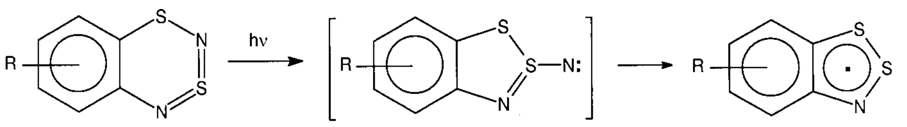

1 - 15

1$^{\bullet}$ **- 15**$^{\bullet}$

Scheme 5

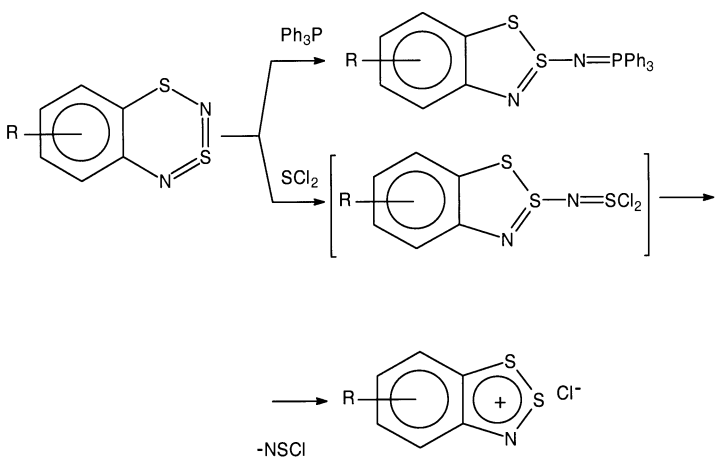

Scheme 6

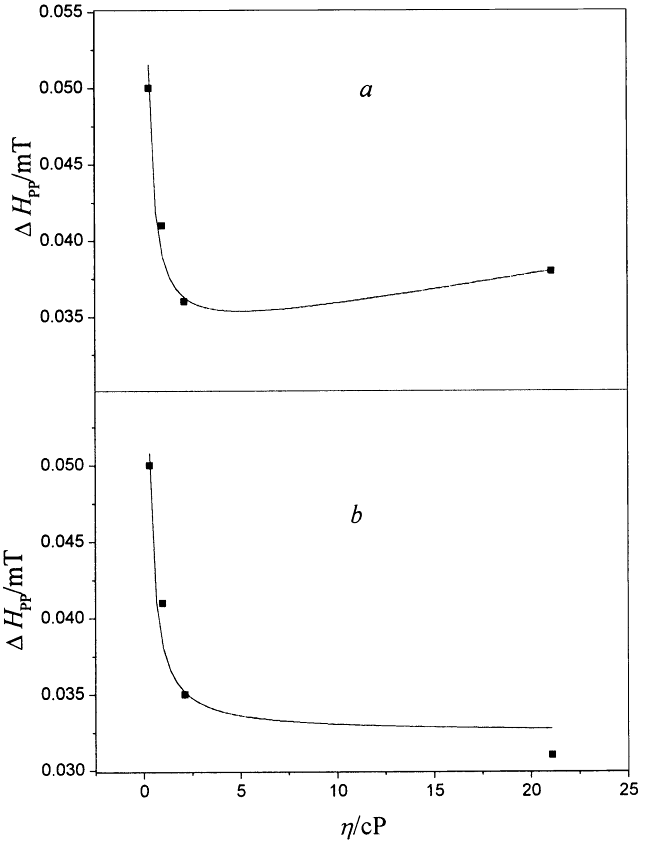

Fig. 7 Dependence of the widths of the lines denoted by asterisks in Fig. 1 on solvent viscosity at 293 K. Dots, experimental data, solid lines, approximation of experimental data by eqn. (2).

contribution of anisotropy modulation by rotation. The optimum values of these parameters are summarized in Table 3.

The contribution of the spin-rotational mechanism to the ESR spectrum linewidth obeys[29] the equation

$$1/T_2 = (12\pi r^3)^{-1} \times [\Delta g\|^2 + 2\Delta g\perp^2] \times (kT/\eta)$$
$$\Delta g\| = g_{zz} - 2.0023$$
$$\Delta g\perp = (g_{xx} + g_{yy})/2 - 2.0023 \qquad (3)$$

where r is the radical radius in the spherical approximation, g_{xx}, g_{yy}, g_{zz}, are the main values of the g-tensor, k is the Boltzman constant, and T is the temperature. The values $g_{xx} = 2.020\,39$, $g_{yy} = 2.010\,75$, $g_{zz} = 1.992\,85$ are determined by simulation of spectrum **1**˙ in frozen squalane at 77 K (Fig. 8). Transforming the second term in eqn. (2) into frequency units and then equating it to eqn. (3), we obtain the value of the radius of **1**˙, $r = 3.8$ Å, corresponding to the geometry of **1**˙ optimized by the B3LYP/6-31G* method. This result agrees with the hypothesis that an increase in the linewidth of the ESR spectra of the title radicals with decreasing solvent viscosity is related to spin-rotational relaxation.

As follows from Table 3, the mechanisms independent of solvent viscosity contribute much to the linewidth. One of these relaxation mechanisms is hfc modulation due to intramolecular motions, for example, the high-amplitude deformation modes of a heterocycle. Although, according to the B3LYP/6-31G* data, radical **1**˙ is flat (Fig. 3), it very likely possesses low-energy deformation modes (with the S2 atom moving out from the heterocycle plane) modulating the hfc and, as a result, leading to broadening of the ESR spectrum lines. Note that, based on the ESR measurements on ^{2}H- and ^{33}S-labelled samples,[30] the bent structure in a solution was proposed for 1,3,2-dithiazolyl radicals (non-fused analogs of radicals **B**, Scheme 1) related to **1**˙–**15**˙. Meanwhile, in the gas phase the planar structure was observed by electron diffraction,[31] which is in agreement with the results of non-empirical quantum chemical calculations.[32] For vibrational modes contributing to the effect, however, the broadening must depend on temperature rather than on solvent viscosity, which requires further study.

Table 3 Optimum values of the parameters a, b, and c in eqn. (2)

Line	a/mT	b/mT cP	c/mT cP^{-1}
Low field	0.0325	0.005 68	0
High field	0.0325	0.005 68	0.000 22

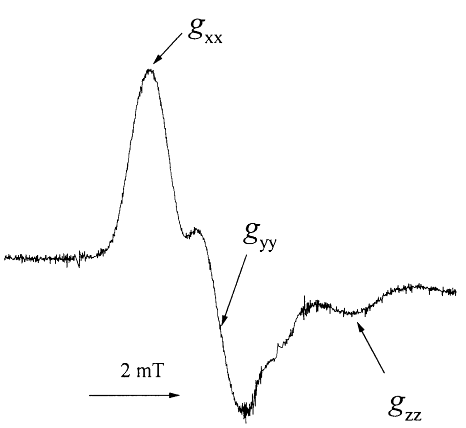

Fig. 8 Spectrum of **1**˙ in squalane at 77 K. The positions of the main values of the g-tensor are marked by arrows.

Acknowledgements

The authors are grateful to the Russian Foundations for Basic Research (Grants 99-03-33115 and 99-03-33158), the State Committee of Higher Education (Goskomvuz) (Grant 3H-218-98), and to the Siberian Branch of Russian Academy of Sciences (Novel Magnetically-Active Systems Project) for financial support.

References

1 *Molecule Based Magnetic Materials. Theory, Techniques and Applications*, ed. M. M. Turnbull, T. Sugimoto and L. K. Thompson, ACS Symposium Series No. 644, American Chemical Society, Washington, DC, 1996.
2 V. I. Ovcharenko and R. Z. Sagdeev, *Russ. Chem. Rev.*, 1999, **68**, 345.
3 J. Zhang, P.M. Lahti and R. Wang, *J. Phys. Org. Chem.*, 1999, **12**, 53.
4 T. Torroba, *J. Prakt. Chem.*, 1999, **341**, 99.
5 T. M. Barclay, L. Beer, A. W. Cordes, R. T. Oakley, K. E. Preuss, N. J. Taylor and R. W. Reed, *J. Chem. Soc., Chem. Commun.*, 1999, 531.
6 F. Palacio, M. Castro, G. Antorrena, R. Burriel, C. Ritter, N. Bricklebank, J. M. Rawson and J. N. B. Smith, *Mol. Cryst. Liq. Cryst.*, 1997, **306**, 293.
7 A. J. Banister and I. B. Gorrell, *Adv. Mater.*, 1998, **10**, 1415.
8 R. Mayer, G. Domschke, S. Bleisch, J. Fabian, A. Bartl and A. Stasko, *Collect. Czech. Chem. Commun.*, 1984, **49**, 684.
9 G. Kirsch, in: *Methoden der Organische Chemie* (*Houben-Weyl*), ed. E. Schaumann, Georg Thieme, Stuttgart, 1994, vol. E8d, p. 10.
10 R. Mayer, A. Bartl and A. Stasko, *Z. Chem.*, 1981, **21**, 264.
11 S. Bleisch, G. Domschke and R. Mayer, *GDR Pat. 138 062DI*, 1979 (*Chem. Abstr.*, 1980, **92**, 128892).
12 R. Mayer, S. Bleisch, G. Domschke and A. Bartl, *Z. Chem.*, 1981, **21**, 146.
13 A. W. Cordes, M. Hojo, H. Koenig, M. C. Noble, R. T. Oakley and W. T. Pennington, *Inorg. Chem.*, 1986, **25**, 1137.
14 A. V. Zibarev, Yu. V. Gatilov and A. O. Miller, *Polyhedron*, 1992, **11**, 1137.

15 I. Yu. Bagryanskaya, Yu. V. Gatilov, A. Yu. Makarov, A. M. Maksimov, A. O. Miller, M. M. Shakirov and A. V. Zibarev, *Heteroatom Chem.*, 1999, **10**, 113.

16 A. Yu. Makarov, I. Yu. Bagryanskaya, Yu. V. Gatilov, T. V. Mikhalina, M. M. Shakirov, L. N. Shchegoleva and A. V. Zibarev, *Heteroatom Chem.*, in the press.

17 (*a*) V. A. Bagryansky, I. V. Vlasyuk, Yu. V. Gatilov, A. Yu. Makarov, Yu. N. Molin, V. V. Shcherbukhin and A. V. Zibarev, *Mendeleev Commun.*, 2000, 5; (*b*) N. P. Gritsan, V. A. Bagryansky, I. V. Vlasyuk, Yu. N. Molin, A. Yu. Makarov and A. V. Zibarev, Conference on Reactive Intermediates and Unusual Molecules, Vienna, Austria, 2000, Book of Abstracts, p. 64.

18 N. P. Gritsan and N. M. Bazhin, *Izv. Akad. Nauk SSSR. Ser. Khim.*, 1981, 280.

19 GAUSSIAN 94, Revision C.3, M. J. Frisch, G. W. Trucks, H. B. Schlegel, P. M. W. Gill, B. G. Johnson, M. A. Robb, J. R. Cheeseman, T. Keith, G. A. Petersson, J. A. Montgomery, K. Raghavachari, M. A. Al-Latam, V. G. Zakrzewsky, J. V. Ortiz, J. B. Foresman, J. Cioslowsky, B. B. Stefanov, A. Nanayakkara, M. Challacombe, C. Y. Peng, P. Y. Ayala, W. Chen, M. W. Wong, L. J. Andres, E. S. Replogle, R. Gomperts, R. L. Martin, D. J. Fox, J. S. Binkley, D. J. Defrees, J. Baker, J. P. Stewart, M. Head-Gordon, C. Gonzales and J. A. Pople, Gaussian Inc., Pittsburgh, PA, 1995.

20 GAUSSIAN 98, Revision A.6, M. J. Frisch, G. W. Trucks, H. B. Schlegel, G. E. Scuseria, M. A. Robb, J. R. Cheeseman, V. G. Zakrzewski, J. A. Montgomery, Jr., R. E. Stratmann, J. C. Burant, S. Dapprich, J. M. Millam, A. D. Daniels, K. N. Kudin, M. C. Strain, O. Farkas, J. Tomasi, V. Barone, M. Cossi, R. Cammi, B. Mennucci, C. Pomelli, C. Adamo, S. Clifford, J. Ochterski, G. A. Petersson, P. Y. Ayala, Q. Cui, K. Morokuma, D. K. Malick, A. D. Rabuck, K. Raghavachari, J. B. Foresman, J. Cioslowski, J. V. Ortiz, B. B. Stefanov, G. Liu, A. Liashenko, P. Piskorz, I. Komaromi, R. Gomperts, R. L. Martin, D. J. Fox, T. Keith, M. A. Al-Laham, C. Y. Peng, A. Nanayakkara, C. Gonzalez, M. Challacombe, P. M. W. Gill, B. Johnson, W. Chen, M. W. Wong, J. L. Andres, C. Gonzalez, M. Head-Gordon, E. S. Replogle and J. A. Pople, Gaussian, Inc., Pittsburgh, PA, 1998.

21 G. Wolmershaeuser, M. Schnauber and T. Wilhelm, *J. Chem. Soc., Chem. Commun.*, 1984, 573.

22 A. V. Zibarev, Yu. V. Gatilov, I. Yu. Bagryanskaya, A. M. Maksimov and A. O. Miller, *J. Chem. Soc., Chem. Commun.*, 1993, 298.

23 R. Mayer, S. Bleisch, G. Domschke, A. Tkac, A. Stasko and A. Bartl, *Org. Magn. Reson.*, 1979, **12**, 532.

24 J. M. Dust and D. R. Arnold, *J. Am. Chem. Soc.*, 1983, **105**, 1221.

25 (*a*) S. Olivella, M. Ballester and J. Castaner, *Tetrahedron Lett.*, 1974, 587; (*b*) S. A. Weiner and G. S. Hammond, *J. Am. Chem. Soc.*, 1969, **91**, 986.

26 E.G. Awere, N. Burford, R.C. Haddon, S. Parsons, J. Passmore, J.V. Warszak and P.S. White, *Inorg. Chem.*, 1990, **29**, 4821.

27 N. P. Gritsan, V. A. Bagryansky, I. V. Vlasyuk, Yu. N. Molin, A. Yu. Makarov and A. V. Zibarev, unpublished work.

28 A. Carrington and A. D. MacLauchlan, *Introduction to Magnetic Resonance*, Evanson, New York, Harper and Row, London, 1967.

29 P. W. Atkins and D. Kivelson, *J. Chem. Phys.*, 1966, **44**, 169.

30 S. A. Fairhurst and L. H. Sutcliffe, *J. Chem. Soc., Faraday Trans. 1*, 1980, 1490.

31 A. G. Awere, N. Burford, C. Mailer, J. Passmore, M. J. Schriver, P. S. White, A. J. Banister, H. Oberhammer and L. H. Sutcliff, *J. Chem. Soc., Chem. Commun.*, 1987, 66.

32 S. M. Matar and A. D. Stephens, *J. Phys. Chem. A*, 2000, **104**, 3718.